



Interfacial micro-structure and properties of dual-layer composite reinforced hollow fiber membranes

Hailiang Liu^{a,*}, Wenshuai Liu^b, Fang Lu^a, Changfa Xiao^a

^aState Key Laboratory of Separation Membranes and Membrane Processes/National Center for International Joint Research on Separation Membranes, School of Material Science and Engineering, Tianjin Polytechnic University, Tianjin 300387, China, Tel. +86 22 8395 5397; emails: liuhailiang723@163.com (H. Liu), 630580687@qq.com (F. Lu), cfxiao@tjpu.edu.cn (C. Xiao)

^bSchool of Textiles, Tianjin Polytechnic University, Tianjin 300387, China, email: 787551878@qq.com

Received 16 May 2017; Accepted 2 October 2017

ABSTRACT

The dual-layer reinforced hollow fiber membranes including separation layer and porous supported matrix were fabricated via dry-wet spinning process. The mixtures of polyvinyl chloride (PVC), polyvinylidene fluoride (PVDF) or polyurethane (PU) polymer solutions were uniformly coated on the surface of the homogeneous PVC matrix membranes, which were prepared by melt-spinning method. The influences of three kinds of polymers on dual-layer reinforced hollow fiber membranes' structure and performance were investigated. Furthermore, the interfacial bonding state of reinforced hollow fiber membranes including the homogeneous-reinforced (HMR) and heterogeneous-reinforced (HTR) interfaces was characterized by indirect method and comparative analysis. The results indicated that a dense interface formed in the PVC reinforced hollow fiber membrane between separation layer and porous supported matrix layer, while no significant interface layer formed in the PVDF and PU reinforced hollow fiber membranes. Moreover, the as-prepared reinforced hollow fiber membranes possessed of a dense and smooth outer surface with no obvious big pores. The permeability of HTR PVDF and PU hollow fiber membranes was better than that of HMR PVC hollow fiber membrane. Specially, the PVC reinforced hollow fiber membrane had a more favorable interfacial bonding state than the PVDF and PU reinforced hollow fiber membranes. By contrast, the tensile strength of as-prepared dual-layer reinforced hollow fiber membranes was all higher than 12 MPa.

Keywords: Dual-layer; Hollow fiber membranes; Reinforced; Tensile strength; Interface

1. Introduction

With the expansion of separation membrane application field, the membrane materials with single compositional substance had already not adapted to the demand of the economic and social development. It was generally accepted that the membrane material with single compositional substance could provide the limited performance under the harsh environment, such as the selective separation performance only provided by the high separation precision membranes or the mechanical property only offered by the

high tensile strength membranes [1–3]. As we all known, the traditional hollow fiber membranes that usually fabricated by immersion-precipitation phase inversion method were easily damaged and broken by the high-pressure water cleaning process or disturbance of the aerated airflow in the membrane bioreactor (MBR) filtration process. In order to adapt to the harsh environment and solve this contradiction of single compositional membranes, the dual-layer hollow fiber membranes could be fabricated by compositing the selective separation layer with the porous supported matrix [2]. Especially, the selective separation layer provided the excellent separation performance, while the porous supported matrix provided the excellent mechanical properties [3].

* Corresponding author.

The research of dual-layer hollow fiber membranes had been reported in the literature largely. Most of these dual-layer hollow fiber membranes were focused on the ultrafiltration [4,5], gas separation [6–8], pervaporation [9], membrane distillation [10,11], nanofiltration [12,13], forward osmosis [14,15], reverse osmosis [16], fuel cell electrode [17] and photocatalytic [18] applications. For instance, the dual-layer hollow fiber membranes could be prepared by one-step co-extrusion method [4,6,9,10,12,17,18], two-step coating method [5,13,16], two-step interfacial polymerization method [15] and multi-layer coating method [8], etc. For these reported methods in the literatures, one-step co-extrusion method exhibited relatively simple preparation process, while the two-step method had widely optional matrix membrane which could be the high tensile strength membrane prepared by melt-spinning cold-stretching method and thermally induced phase separation method. All these researches were focused on the permeability and mechanical properties. However, the researchers rarely investigated the interfacial bonding state of the prepared dual-layer hollow fiber membranes, systematically. Specially, the interfacial bonding state between the separation layer and the porous supported matrix played an important role in the dual-layer membranes in terms of the service life of the membranes in the membrane separation system. Moreover, the good interfacial bonding strength could avoid the peeling off of the separation layer from the porous supported matrix by the high-pressure hydraulic cleaning process or disturbance of the aerated air-flow, such as the MBR filtration process. However, the conventional reinforced hollow fiber membranes could provide limited interfacial bonding strength, because of the poor compatibility between separation layer and support layer, such as polyester tubular braid reinforced PVDF hollow fiber membranes. Thus, the good interfacial bonding state was a primary requirement for the effective use of supported matrix properties so as to ensure the load transfer from the outer layer to the supported matrix [19].

There was no denying that the transverse and longitudinal strength of the composite materials were closely related to the interfacial bonding strength. Generally, there were two methods to characterize the interfacial bonding state of the composite materials in the literatures, such as the large specimen macromechanical tests that described as the interlaminar shear strength [20] and the single fiber micromechanical test that described as the single fiber pull-out test [21]. However, there were many difficulties to test the interfacial bonding strength of the dual-layer hollow fiber membranes by the aforementioned methods. In general, the separation layer of the dual-layer hollow fiber membranes was thin. Thus, we attempted to characterize the interfacial bonding strength of the dual-layer hollow fiber membranes by indirect method and comparative analysis in our previous study [22]. Furthermore, the constant stretching method was utilized to determine the permeability and separation properties of prepared reinforced membrane, which were associated with the separation layer and the interface to a large extent. In the constant stretching process, the pure water flux (PWF) and rejection might increase along with the broken interface. Hence, the variation of the PWF and rejection after stretching could reflect the reinforced hollow fiber membranes' change of the interfacial bonding state, indirectly [22].

In this study, dual-layer PVC, PVDF and PU reinforced hollow fiber membranes were prepared by coating the PVC, PVDF and PU polymer solutions on the PVC hollow fiber matrix membrane via the co-solvent method. The PVC hollow fiber matrix membranes were fabricated by melt-spinning method. The influences of three polymer types on structure and performance of dual-layer reinforced hollow fiber membranes were investigated by morphology observation, permeability and mechanical property measurements. Furthermore, the interfacial bonding state of three reinforced hollow fiber membranes was characterized by indirect method and comparative analysis for the changes of PWF and rejections after constant stretching process.

2. Experimental

2.1. Materials

Polyvinyl chloride (PVC, fiber grade, DG-1000k, the average degree of polymerization is $1,030 \pm 50$) resin was purchased from Tianjin Dagu Chemical Plant (Tianjin, China). Polyvinylidene fluoride (PVDF, Solef 6010) was supplied by Solvay Co., Ltd. (Belgium). Polyurethane (PU, polyether-type, the molecular weight of polyether is 1,000, fiber grade, polyether/diisocyanate/butanediol = 1/2/1) was purchased from Tianjin Daqiu Zhuang Foamy Factory (Tianjin, China). Dioctyl phthalate (DOP, >99.5%) was obtained from Tianjin Kermel Chemical Reagent Co., Ltd. N,N-dimethylacetamide (DMAc, Analytical Reagent) and polyvinylpyrrolidone (PVP, Analytical Reagent, K30, Mw = 10,000) were bought from Tianjin Guangfu Fine Chemical Research Institute (Tianjin, China). Bovine serum albumin (BSA, Analytical Reagent, Mw = 68,000) was supplied from Beijing Aoboxing Universeen Bio-tech Co., Ltd. (Beijing, China).

2.2. Fabrication of dual-layer reinforced hollow fiber membranes

First, the PVC hollow fiber matrix membranes were prepared by melt-spinning method. The preparation steps were mentioned in our previous literature [2]. And then, the prepared PVC hollow fiber matrix membranes were washed in ethanol for at least 48 h to leach out the DOP completely. After the DOP extraction, the membranes were washed by deionized water to leach out the residual ethanol. Finally, the PVC hollow fiber matrix membranes were prepared.

Besides, the dual-layer reinforced hollow fiber membranes were fabricated via dry-wet spinning process. The schematic diagram of the coating system is shown in Fig. 1. In the preparation process, the polymer solutions were obtained by blending PVC or PVDF or PU (10 wt%), PVP (10 wt%) and DMAc (80 wt%) under constant mechanical stirring in a three-necked round-bottom flask for 4 h at 70°C. And then, the PVC matrix membrane went through the coating device in order to coat the polymer solutions on the PVC matrix membrane outer surface. Next, the PVC matrix membrane with coating polymer solutions came into coagulation bath. After the formation of the dual-layer reinforced hollow fiber membranes, the prepared membranes were stored in water for at least 48 h to remove the residual solvents. In the end, the dual-layer reinforced hollow fiber membranes were obtained. The spinning parameters of dual-layer reinforced hollow fiber membranes are shown in Table 1.

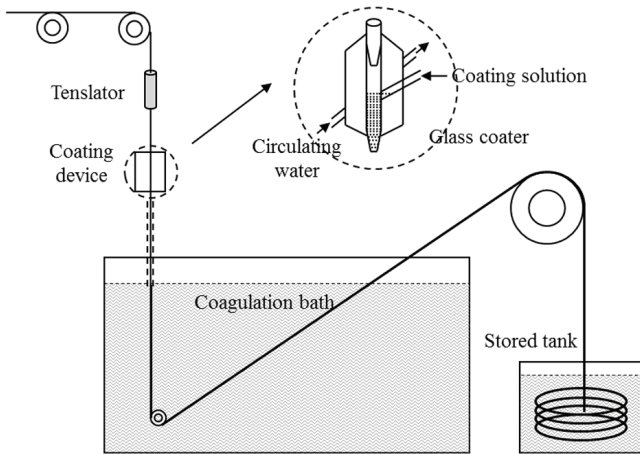


Fig. 1. Schematic diagram of the coating system.

Table 1
Spinning parameters of dual-layer reinforced hollow fiber membranes

Spinning conditions	Value
Matrix membrane	PVC hollow fiber membrane
Mixing temperature/°C	70.0
Spinning temperature/°C	20.0
External coagulation	Water
External coagulation T/°C	20.0 ± 2.0
Air gap/cm	8.0
Take up speed/m×min ⁻¹	2.2

2.3. Membrane characterizations

2.3.1. Morphology observation

Scanning electron microscope (SEM, Quanta 200, Netherlands FEI) was utilized to investigate the morphology of as-prepared hollow fiber membranes' surface and cross-section. The membranes were immersed in liquid nitrogen for 10–15 s so as to freeze. Then the frozen membranes were broken for cross-section observation. Samples were all gold sputtered before testing.

2.4. Permeation performance experiments

The schematic diagram of filtration experimental setup was shown in Fig. 2. All experiments were performed in hollow fiber modules. The effective membrane area of each membrane module was 26.0 cm² in this test.

The PWF (J_0) was measured with hollow fiber membranes at 0.1 MPa pressure under the condition of outside pressure and was calculated by Eq. (1):

$$J = \frac{V}{At} \quad (1)$$

where J is the permeate flux of membrane (L m⁻² h⁻¹), V is the quantity of permeation (L), A is the effective area of membrane (m²) and t is the testing time (h).

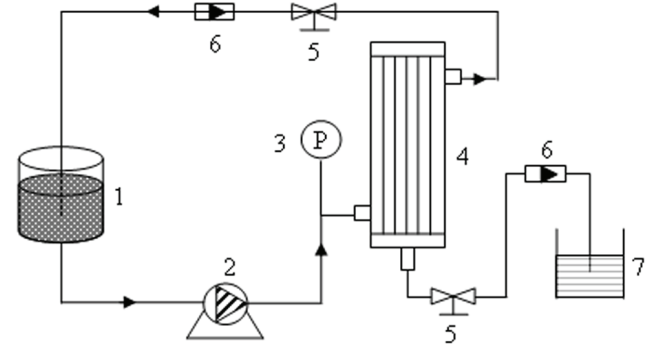


Fig. 2. Schematic diagram of filtration system: (1) feed tank, (2) feed pump, (3) manometer, (4) membrane cell, (5) control valve, (6) rotameter and (7) permeate tank.

The filtration experiments were then carried out by 1 g L⁻¹ BSA solution. The protein permeation flux (PPF) for the BSA solution was recorded as J_1 based on the water quantity permeating the membranes at the same pressure of 0.1 MPa and was calculated by Eq. (1). The rejection (R) of the protein was defined by Eq. (2):

$$R = \left(1 - \frac{C_p}{C_f} \right) \times 100\% \quad (2)$$

where C_f and C_p are the concentration of protein in the feed and the permeate solution, respectively. The concentration of feed solution and permeate solution were determined by UV spectroscopy at wavelength of 280 nm, using a PERSEE TU-1901 spectrophotometer (Beijing Purkinje General Instrument Co., Ltd., Beijing, China).

After 60 min of filtration experiment, the membrane was washed to recover its permeability. The washing process continued for 10 min. After that, the membrane recovery flux (J_2) was measured for 30 min by deionized water and was calculated by Eq. (1).

In order to analyze the antifouling property in details, several ratios were defined. The flux recovery rate (FR), total flux decline ratio (DR_t), reversible flux decline ratio (DR_r), irreversible flux decline ratio (DR_{ir}) were defined and calculated as follows [22–24]:

$$FR = \frac{J_2}{J_0} \times 100\% \quad (3)$$

$$DR_t = \left(1 - \frac{J_1}{J_0} \right) \times 100\% \quad (4)$$

$$DR_r = \left(\frac{J_2 - J_1}{J_0} \right) \times 100\% \quad (5)$$

$$DR_{ir} = \left(1 - \frac{J_2}{J_0} \right) \times 100\% \quad (6)$$

Here, the higher value of FRR and lower value of DR_t indicated the better antifouling properties of the membranes.

2.5. Apparent viscosity of the polymer solutions

The viscosities of the casting solutions with different polymers (PVC, PVDF or PU) were determined at temperature from 15°C to 80°C by a rotational viscometer (SNB-1, Shanghai FangRui Instrument Co., Ltd., Shanghai, China).

2.6. Infiltration properties of polymer solutions

The infiltration properties of the membrane were investigated by the contact angle between the polymer solution and the membrane surface. The contact angle was measured by a contact angle measuring instrument (DSA100, KRUSS, Germany). The measurements were carried out at 25°C (relative humidity: 50%). A drop of the polymer solution was dropped on the outer surface of the sample, then a video was created. The different images from the video determined the contact angle at the different time. Each sample was measured five times at different area of the membrane to evaluate the average value. Then the change ratios of the contact angle at t time when compared with that at 0 s could be defined as follows:

$$\text{Ratio}(t) = \frac{\theta_0 - \theta_t}{\theta_0} \times 100\% \quad (7)$$

where θ_0 is the contact angle at time 0 s, θ_t is the contact angle at time t .

2.7. Measurement of mechanical property

At room temperature, mechanical properties of dual-layer reinforced hollow fiber membranes were measured by a universal mechanical testing machine (CMT4204, MTS Systems, China). The gripping range and the tensile rate were 100 mm and 100 mm min^{-1} , respectively. Each sample was tested five times to evaluate the average value.

3. Results and discussion

3.1. Infiltration properties of polymer solutions

Generally, during the preparation of composite materials, one phase contacted with the other phase of the liquid or molten states in the two phases of the composite materials, and then combined with each other for the curing reaction. The adhesion action referred to two kinds of forces existing at the interface of these two materials, which were the physical force and the chemical force [3]. The physical force mainly contained mechanical wedging and adhesive curing, while the chemical force was mainly described as the chemical bond action between two phases of composite materials. In this study, there was no chemical bonds combination between the polymer solution and reinforced matrix membrane of the reinforced hollow fiber membranes, but only existed with the molecular interactions as the polar groups or molecular chain segments of the materials to be closed to each other. Both of these two forces were closely related to the surface roughness

of the reinforcement and the diffusion degree of the polymer solutions to the matrix membrane. Poor infiltration between the polymer solutions and the matrix membrane easily led to defects or stress concentration phenomenon near the interface so as to reduce the interfacial bonding strength. On the contrary, favorable infiltration performance could improve the interfacial bonding strength significantly. The contact angle measurement was usually utilized to characterize the infiltration ability [25]. The smaller the contact angle between the matrix membrane and the polymer solutions was, the better the infiltration performance was at the same contact time.

The apparent viscosity of PVC, PVDF and PU casting solutions is shown in Fig. 3. It could be seen that the apparent viscosity of PU casting solution was obviously higher than that of the PVC and PVDF casting solutions, but the apparent viscosity of the PVC and PVDF casting solutions was nearly the same at the same polymer concentration and membrane fabrication temperature from Fig. 3. The high apparent viscosity would decrease the infiltration and diffusion performance of the polymer solution to the matrix membrane at the spinning process.

Fig. 4 shows the contact angle and its change rate of the PVC, PVDF and PU casting solutions with same concentration to the outer surface of PVC hollow fiber matrix membrane at the temperature of 25°C. From Fig. 4(a), the contact angle of the PVDF and PU casting solutions were higher than that of the PVC casting solution when the casting solution just contacted the outer surface of PVC hollow fiber matrix membrane ($t = 0$ s). The results could be attributed that the infiltration performance of the PVC casting solution to the PVC hollow fiber matrix membrane was better than that of the PVDF and PU casting solutions. All of the contact angles of PVC, PVDF and PU casting solutions to the PVC hollow fiber matrix membrane decreased with the prolonging of the contact time from Fig. 4(a). After 10 s, the stable value of the contact angle for these three casting solutions was nearly the same, which was attributed to the viscosity of these casting solutions. Combined with Fig. 4(b), the change rate of the contact angle at 10 s increased less than the change rate of the contact angle at 5 s. This indicated that the effect on the diffusion mainly occurred at the first few seconds as the

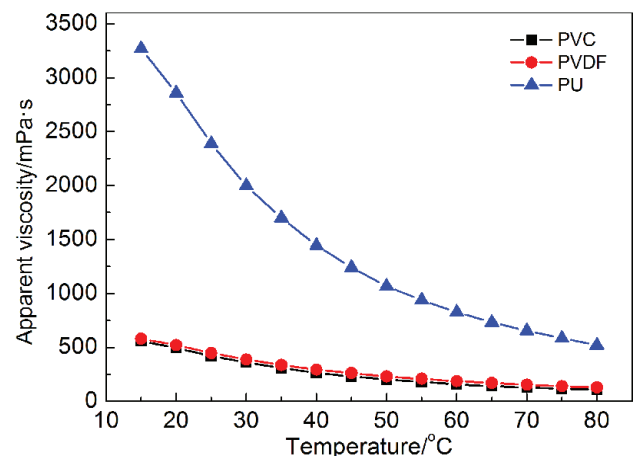


Fig. 3. Effects of temperature on apparent viscosity of PVC, PVDF and PU casting solutions.

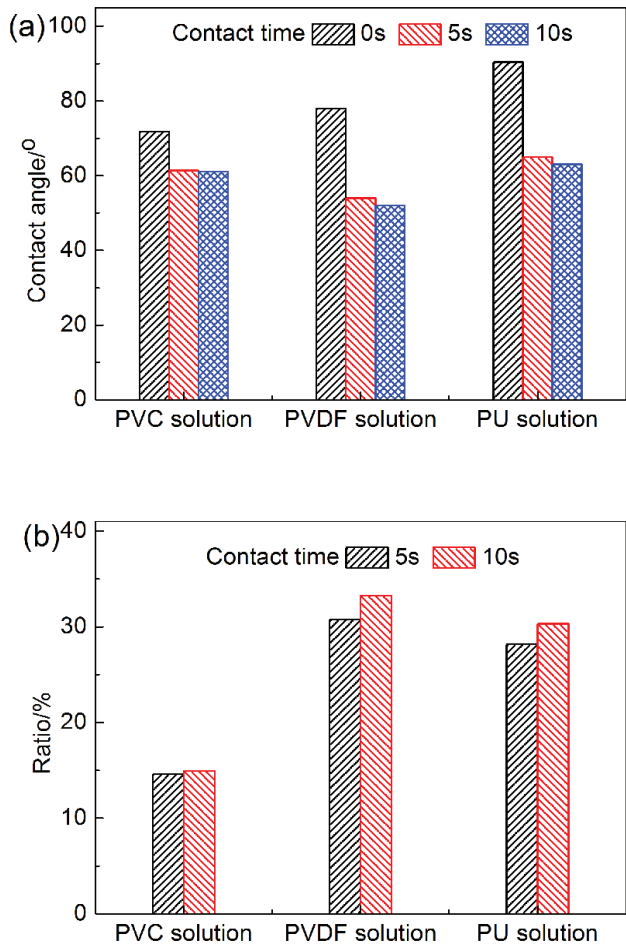


Fig. 4. Contact angle (a) and its change rate (b) of PVC, PVDF and PU casting solutions on PVC hollow fiber matrix membrane. ($T = 20^{\circ}\text{C}$).

casting solution contacting the matrix membrane. Therefore, the appropriate contacting time of the casting solution to the matrix membrane not only obtained the best infiltration effect on the matrix membrane but also reduced the swelling and dissolving of the PVC hollow fiber matrix membrane which could guarantee to enhance the mechanical properties of the reinforced membranes.

3.2. Morphology of dual-layer reinforced hollow fiber membrane

The cross sectional and outer surface morphologies of as-prepared PVC matrix membrane and PVC, PVDF and PU reinforced hollow fiber membranes are shown in Fig. 5. The characterization of the dual-layer reinforced hollow fiber membranes is tabulated in Table 2. Fig. 5(a1) shows that the PVC hollow fiber matrix membrane was a kind of homogeneous membrane and possessed of a sponge-like structure. Moreover, the pores on the outer surface were long and narrow observing from Fig. 5(a2). It also can be seen that the prepared reinforced hollow fiber membranes consisted of the separation layer and the porous supported matrix layer from Fig. 5. Furthermore, Fig. 5(b1) shows that the pores in the separation layer were typical finger-like structure for the PVC reinforced hollow fiber membrane of M1, and a dense interface formed between the separation layer and the porous supported matrix layer. When the PVDF casting solution was used as the separation layer, the pores in the separation layer were the irregular macroporous structure and turned to the regular sponge-like structure from outer to inner of the separation layer for M2 from Fig. 5(c1). The pore size became smaller from outer to inner in the sponge-like structure for M2. Specially, there were obviously space between the separation layer and the porous supported matrix layer, as well as formed the layered structure for M2. From Fig. 5(d1), the separation layer of PU reinforced hollow fiber membranes for M3 show the irregular big porous structure. From Figs. 5(b2), (c2) and (d2), the prepared reinforced hollow fiber membranes

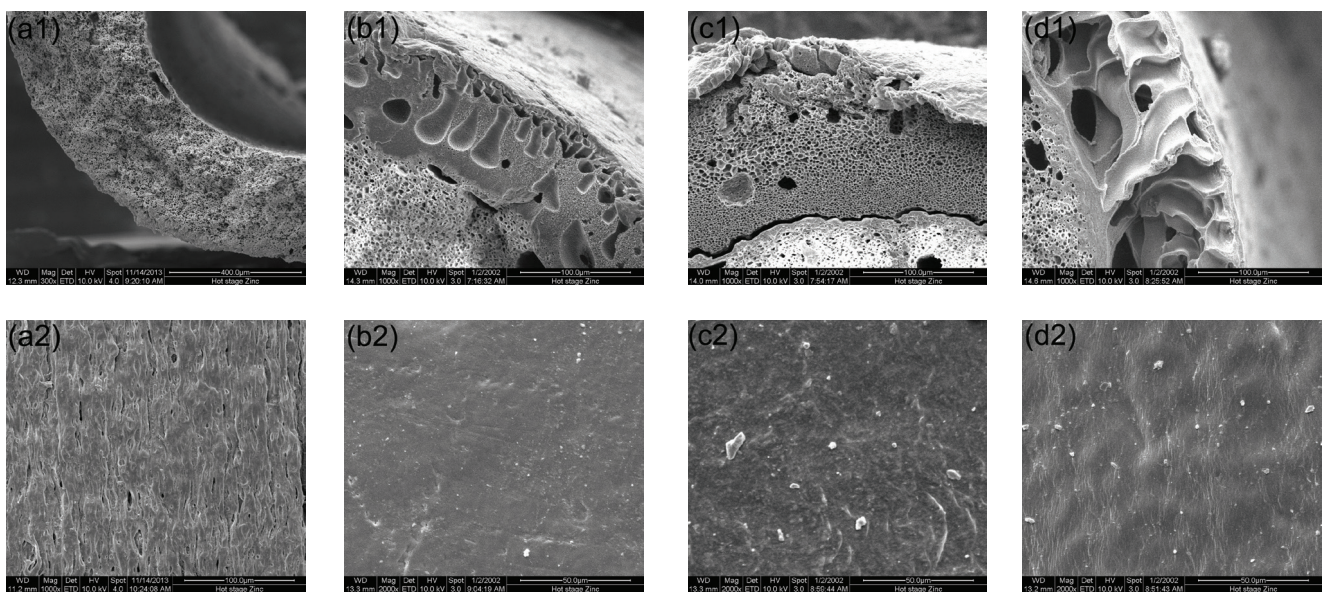


Fig. 5. Cross sectional and outer surface morphologies of PVC matrix membrane and PVC, PVDF and PU reinforced hollow fiber membranes ((a)-M0, (b)-M1, (c)-M2, (d)-M3).

Table 2
Characterization of dual-layer reinforced hollow fiber membranes (OD: outer diameter, ID: inner diameter)

Membrane ID	OD/mm	ID/mm	Wall thickness/mm	Separation layer thickness/mm
M0	1.356 ± 0.021	0.752 ± 0.016	0.302	0
M1	1.522 ± 0.017	0.753 ± 0.037	0.385	0.082 ± 0.012
M2	1.589 ± 0.041	0.774 ± 0.014	0.408	0.086 ± 0.029
M3	1.467 ± 0.013	0.713 ± 0.055	0.377	0.105 ± 0.020

Table 3
Solubility parameter of polymers [26]

	$\delta_d/(\text{J}\cdot\text{cm}^{-3})^{1/2}$	$\delta_p/(\text{J}\cdot\text{cm}^{-3})^{1/2}$	$\delta_r/(\text{J}\cdot\text{cm}^{-3})^{1/2}$	$\delta/(\text{J}\cdot\text{cm}^{-3})^{1/2}$
PVC	18.72	10.03	3.07	21.46
PVDF	17.20	12.50	9.20	23.20
PU	–	–	–	20.5

possess of a dense and smooth outer surface with no obvious big pores. The outer surface of PVC reinforced hollow fiber membrane was smoother than that of the PVDF reinforced hollow fiber membrane by comparing Figs. 5(b2) and (c2). Also, the outer surface of PU reinforced hollow fiber membrane appeared the fold with fine lines from Fig. 5(d2).

The solubility parameter of PVC, PVDF and PU is shown in Table 3, respectively [26]. According to the data in Table 3, $\Delta\delta_1 = |\delta_{\text{PVC}} - \delta_{\text{PVDF}}| = 1.76 (\text{J}\cdot\text{cm}^{-3})^{1/2}$ and $\Delta\delta_2 = |\delta_{\text{PVC}} - \delta_{\text{PU}}| = 0.96 (\text{J}\cdot\text{cm}^{-3})^{1/2}$. Generally, if $\Delta\delta > 1.0 (\text{J}\cdot\text{cm}^{-3})^{1/2}$, the compatibility of the two polymer would be bad, and the chains of the two polymer would exclude each other. Thus, the compatibility of PVC and PVDF would be poorer than that of PVC and PU, and chains of the PVC and PVDF would be mutually exclusive [27,28]. Though the apparent viscosity and contact angle of PVDF casting solution were lower than that of PU casting solution from Figs. 3 and 4, the space would be easier to form at the thin interfacial layer between PVC and PVDF than that between PVC and PU during sample preparation process. The results indicated that the attachment of PVDF to the PVC hollow fiber matrix membrane was worse than that of PU, which was caused by the poor compatibility of these two polymers.

The interfacial bonding strength between the separation layer and the porous supported matrix layer was not only related to the infiltration of the polymer solution to the matrix membrane but also related to the swelling and dissolving of the matrix membrane that caused by DMAc in the polymer solution, and the compatibility of the polymer in the casting solution and the matrix membrane. Combined with the SEM morphologies in Fig. 5, the schematic diagram of polymer macromolecule chain entanglement in the reinforcement process is shown in Fig. 6. The macromolecule chain structure on the outer surface of PVC hollow fiber matrix membrane is described as Fig. 6(a). When the casting solution contacted the PVC hollow fiber matrix membrane, the macromolecule would be swelling even dissolving, and then the gap between the macromolecule chains increased as shown in Fig. 6(b). When the polymers in the casting solution were

the same as the matrix membrane, the reinforced process was described as the homogenous-reinforced (HMR) process (II), otherwise, it was described as the heterogeneous-reinforced (HTR) process (III). In the HMR process, the entanglement of the PVC macromolecule chains in the casting solutions and the matrix membrane occurred, due to the interface diffusion. Moreover, the same material in the casting solution and matrix membrane could avoid the phenomenon of thermodynamic incompatibility between different kinds of materials, made its degree of entanglement higher after curing of the reinforced membrane which formed the compact interface structure as shown in Fig. 6(c). In the HTR process, the thermodynamic incompatibility of the different kinds of materials in the separation layer and matrix membrane decreased the degree of entanglement between the PVDF or PU macromolecule chains in casting solutions and PVC macromolecule chains in matrix membrane which formed the loose interface structure as shown in Fig. 6(d). Generally, the loose interface structure would decrease the interfacial bonding strength which easily led to the peeling off of the separation layer from matrix membrane.

3.3. Membrane permeation and antifouling property

It was known to all that the filtration performance including the permeation, rejection and antifouling properties (including FR, DR_v , DR_r and DR_{ir}) of the prepared reinforced hollow fiber membranes was evaluated in cross-flow filtration mode employing BSA aqueous solution as model feed solution. The DR_{ir} was caused by the irreversible adsorption and adhesion of protein on membrane surface and inner pores (irreversible fouling), which would not be recovered by hydraulic cleaning. On the contrary, DR_r was caused by the reversible protein deposition and weak interaction of protein on membrane surface (reversible fouling), which would be recovered by hydraulic cleaning. Moreover, the FR was the characteristic parameter of membrane antifouling property [24]. In general, the higher value of FR and lower value of DR_r indicated the better antifouling properties of the membranes.

Similarly, the permeation properties of prepared PVC, PVDF and PU reinforced hollow fiber membranes such as PWF, PPF and protein rejections are shown in Table 4. It can be seen from Fig. 7, the time-dependent permeation flux of the prepared reinforced hollow fiber membranes and the summary of the corresponding FR, DR_v , DR_r , DR_{ir} values during the BSA solution filtration, individually. From Table 4 and Fig. 7(a), the PWF of M0 membrane decreased dramatically with the prolonging of operation time, but the PWF of M1, M2 and M3 membranes maintained stable during the

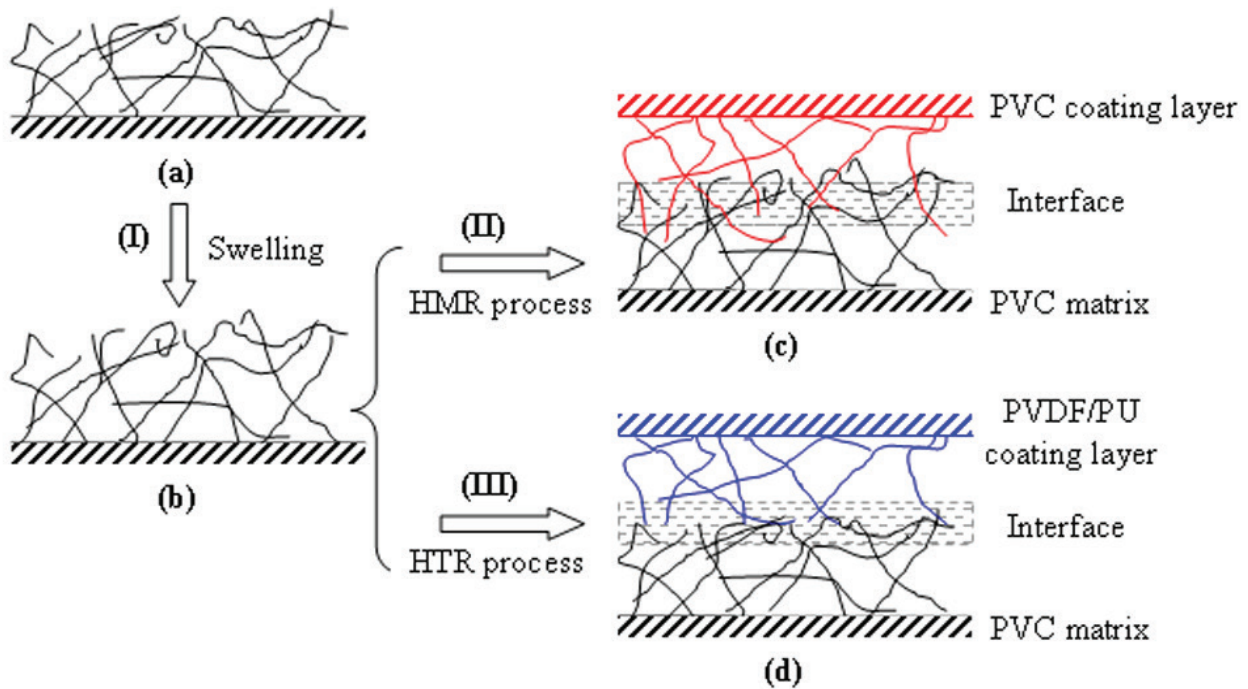


Fig. 6. Schematic diagram of polymer macromolecule chain entanglement in the reinforcement process.

Table 4
Permeation properties of dual-layer reinforced hollow fiber membranes (operating pressure: 0.1 MPa, testing temperature: 20°C ± 2°C)

Membrane ID	PWF (J_0)/L·m ⁻² ·h ⁻¹	PPF (J_1)/L·m ⁻² ·h ⁻¹	Rejection/%
M0	28.23 ± 3.91	6.09 ± 0.78	13.89 ± 5.30
M1	30.27 ± 0.68	23.07 ± 2.72	92.25 ± 1.48
M2	96.87 ± 2.02	75.95 ± 0.58	72.65 ± 0.50
M3	58.87 ± 1.24	44.37 ± 0.62	95.32 ± 0.17

PWF test process. This could be explained by the fact that the existence of the dense skin layer could improve the compaction resistance of the membrane. After 30 min filtration, the stable PWF of M0 membrane was lower than that of M1, M2 and M3 membranes, while the PWF of M2 and M3 membranes was higher than that of M1 membrane. This could be explained by the fact that the forming of the dense interface for M1 increased the membrane resistance. From Table 4, the rejection of prepared reinforced membranes was higher than that of PVC hollow fiber matrix membrane. This was due to the formation of dense skin layer during the preparation process of reinforced hollow fiber membranes (Fig. 5).

From Fig. 7(b), the M0 membrane exhibited poor FR and relative high DR_v with the DR_r as high as 72.5%. The undesirable adsorption and pores blocking of protein took place in the inner pores of M0 membrane which had a porous outer surface with obvious open pores during BSA solution filtration. The FR of the reinforced hollow fiber membranes was elevated to 79.4%, 85.2% and 76.1% for M1, M2 and M3 from

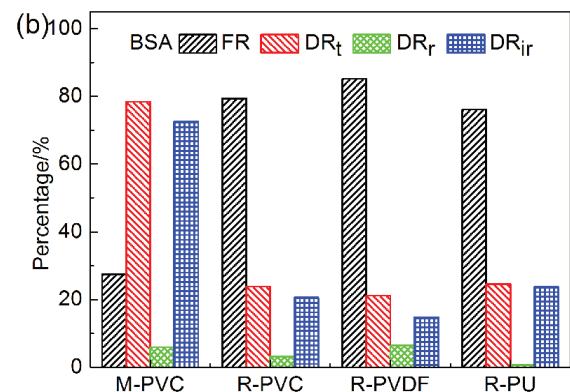
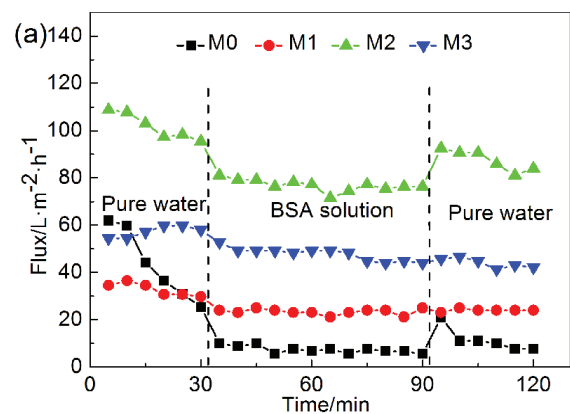


Fig. 7. Time-dependent permeate flux of M0, M1, M2 and M3 membranes (a) and the summary of the corresponding FR, DR_v, DR_t, DR_r values (b) during BSA solution filtration.

27.5% for M0 membrane, respectively, which indicated that the reinforced method could improve the antifouling property of the PVC hollow fiber matrix membrane. The value of DR_{ir} was nearly to the value of DR_r , which indicated that the irreversible adsorption and adhesion of protein on PVC membranes were the main reasons for decline of the flux during the BSA solution filtration process from Fig. 7(b).

3.4. Mechanical performance

The tensile strength and elongation at break of PVC, PVDF and PU reinforced hollow fiber membranes are shown in Fig. 8. It can be seen that all of the tensile strength of reinforced membranes is higher than 12 MPa, while it is lower than the PVC hollow fiber matrix membrane (M0). Generally, the tensile strength of PVC matrix reinforced hollow fiber membranes mainly depended on the PVC hollow fiber matrix membrane. In the coating process, the dissolution of the PVC hollow fiber matrix membrane in the polymer solution with high concentration of DMAc solvent, which might reduce the tensile strength of PVC, PVDF and PU reinforced hollow fiber membranes. Moreover, the formation of the dense interface could improve the tensile strength to some extent. Thus, the tensile strength of M1 membrane was higher than that of M2 and M3 membranes.

3.5. Interfacial bonding state

In this study, the PVC, PVDF and PU reinforced hollow fiber membranes were stretched at a constant speed of 1 mm min^{-1} . The elongation ratio was set as 2%, 5%, 10% and 20% until breakage. According to the variation PWF and protein rejection of these dual-layer reinforced hollow fiber membranes after elongation, the interfacial bonding state could be evaluated. Fig. 9 shows the variation PWF and protein rejection of M1, M2 and M3 membranes with elongation ratio. From Fig. 9, the PWF of M1 membrane changed slightly, while the protein rejection first decreased slightly and then remained stable with the increase of elongation ratio. This indicated that the changes of M1 membrane structure were not obvious and the M1 membrane exhibited a favorable interfacial bonding state. The protein rejection of M2 membrane was nearly to the un-stretched membrane at the elongation ratio of 2%, but the PWF increased dramatically. This indicated that the pores on outer surface were almost unchanged and the increase of PWF was mainly caused by the damage of interface. With the increase of elongation ratio from 2% to 10%, the PWF increased and the protein rejection decreased. This reason could be attributed that the interface was damaged and pore size on outer surface increased. When the elongation ratio was higher than 10%, both of the PWF and protein rejection of M2 membrane changed slightly. Fig. 10 shows that the outer layer of M2 had peeled off from the matrix layer when the membrane broke down after tensile strength test. These changes indicated that the M2 membrane possessed of a poor interfacial bonding state. Moreover, the PWF and protein rejection of M3 membrane changed slightly with the increase of elongation ratio when the elongation was less than 20%. But the PWF increased, while protein rejection decreased obviously when it was breakage, which indicated that the interfacial bonding

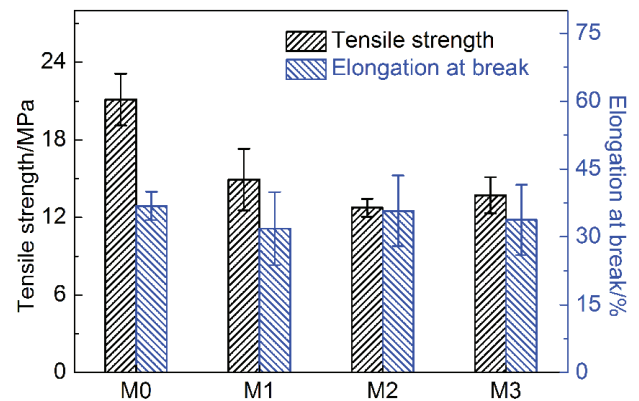


Fig. 8. Mechanical properties of dual-layer reinforced hollow fiber membranes.

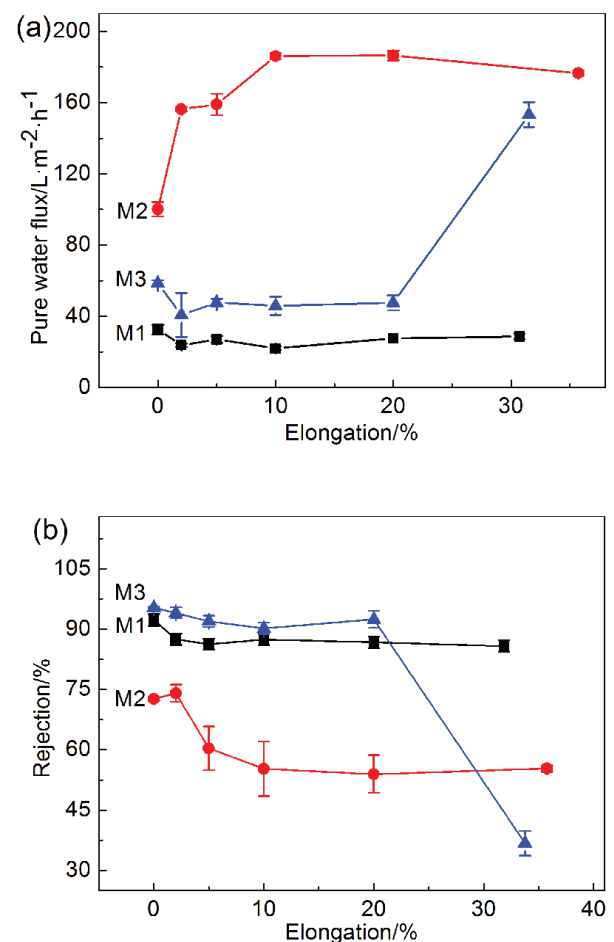


Fig. 9. Variation PWF and protein rejection of M1, M2 and M3 membranes with elongation ratio (testing temperature: 20°C).

state was damaged at the same time. These changes indicated that the M3 membrane exhibited a good interfacial bonding state when the elongation was less than 20%.

With the analysis above, we concluded that the PVC reinforced hollow fiber membranes (M1) with HMR interface

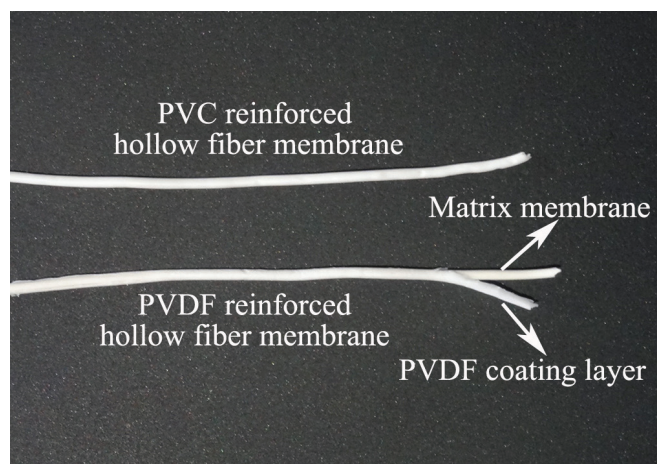


Fig. 10. Picture of M1 and M2 membranes after tensile strength test.

exhibited a more favorable interfacial bonding state than the PVDF and PU reinforced hollow fiber membranes with HTR interface (M2, M3).

4. Conclusion

The dual-layer PVC, PVDF and PU reinforced hollow fiber membranes including separation layer and porous supported matrix were fabricated via dry-wet spinning process. Specially, a dense interface formed in the PVC reinforced hollow fiber membrane between separation layer and porous supported matrix layer, while no significant interface layer formed in the PVDF and PU reinforced hollow fiber membrane. The as-prepared reinforced hollow fiber membranes possessed of a dense and smooth outer surface with no obvious big pores. Moreover, the permeability of HTR PVDF and PU hollow fiber membranes was better than that of HMR PVC hollow fiber membranes. The PVC reinforced hollow fiber membranes with HMR interface exhibited a more favorable interfacial bonding state than the PVDF and PU reinforced hollow fiber membranes with HTR interface. The tensile strength of prepared dual-layer reinforced hollow fiber membranes was all higher than 12 MPa.

Acknowledgments

The authors gratefully acknowledge the research funding provided by the National Natural Science Foundation of China (51603146, 21274109), the Science and Technology Plans of Tianjin (No.15PSTYJC00240).

References

- [1] L. Setiawan, R. Wang, L. Shi, K. Li, A.G. Fane, Novel dual-layer hollow fiber membranes applied for forward osmosis process, *J. Membr. Sci.*, 421 (2012) 238–246.
- [2] H.L. Liu, C.F. Xiao, Q.L. Huang, X.Y. Hu, Structure design and performance study on homogeneous-reinforced polyvinyl chloride hollow fiber membranes, *Desalination*, 331 (2013) 35–45.
- [3] X.L. Zhang, C.F. Xiao, X.Y. Hu, Q.Q. Bai, Preparation and properties of homogeneous-reinforced polyvinylidene fluoride hollow fiber membrane, *Appl. Surf. Sci.*, 264 (2013) 801–810.
- [4] Y. Li, T.S. Chung, Exploration of highly sulfonated polyethersulfone (SPES) as a membrane material with the aid of dual-layer hollow fiber fabrication technology for protein separation, *J. Membr. Sci.*, 309 (2008) 45–55.
- [5] T.Y. Liu, R.X. Zhang, Q. Li, B.V.D. Bruggen, X.L. Wang, Fabrication of a novel dual-layer (PES/PVDF) hollow fiber ultrafiltration membrane for wastewater treatment, *J. Membr. Sci.*, 472 (2014) 119–132.
- [6] X.L. Ding, Y.M. Cao, H.Y. Zhao, L.N. Wang, Q. Yuan, Fabrication of high performance matrimid/polysulfone dual-layer hollow fiber membranes for O₂/N₂ separation, *J. Membr. Sci.*, 323 (2008) 352–361.
- [7] S.S. Hosseini, N. Peng, T.S. Chung, Gas separation membranes developed through integration of polymer blending and dual-layer hollow fiber spinning process for hydrogen and natural gas enrichments, *J. Membr. Sci.*, 349 (2010) 156–166.
- [8] H.Z. Chen, Y.C. Xiao, T.S. Chung, Multi-layer composite hollow fiber membranes derived from poly(ethylene glycol) (PEG) containing hybrid materials for CO₂/N₂ separation, *J. Membr. Sci.*, 381 (2011) 211–220.
- [9] Y. Wang, S.H. Coh, T.S. Chung, P. Na, Polyamide-imide/polyetherimide dual-layer hollow fiber membranes for pervaporation dehydration of C1-C4 alcohols, *J. Membr. Sci.*, 326 (2009) 222–233.
- [10] S. Bonyadi, T.S. Chung, Flux enhancement in membrane distillation by fabrication of dual layer hydrophilic-hydrophobic hollow fiber membranes, *J. Membr. Sci.*, 306 (2007) 134–146.
- [11] P. Wang, M.M. Tioh, T.S. Chung, Morphological architecture of dual-layer hollow fiber for membrane distillation with higher desalination performance, *Water Res.*, 45 (2011) 5489–5500.
- [12] S.P. Sun, K.Y. Wang, N. Peng, T.A. Hatton, T.S. Chung, Novel polyamide-imide/cellulose acetate dual-layer hollow fiber membranes for nanofiltration, *J. Membr. Sci.*, 363 (2010) 232–242.
- [13] Y. Zhang, R. Mulvenna, B.W. Boudouris, W.A. Phillip, Nanomanufacturing of high-performance hollow fiber nanofiltration membranes by coating uniform block polymer films from solution, *J. Mater. Chem. A*, 5 (2017) 3358–3370.
- [14] Q. Yang, K.Y. Wang, T.S. Chung, Dual-layer hollow fibers with enhanced flux as novel forward osmosis membranes for water production, *Environ. Sci. Technol.*, 43 (2009) 2800–2805.
- [15] L. Setiawan, R. Wang, K. Li, A.G. Fane, Fabrication and characterization of forward osmosis hollow fiber membranes with antifouling NF-like selective layer, *J. Membr. Sci.*, 394–395 (2012) 80–88.
- [16] T.Y. Liu, C.K. Li, B. Pang, B.V.D. Bruggen, X.L. Wang, Fabrication of a dual-layer (CA/PVDF) hollow fiber membrane for RO concentrate treatment, *Desalination*, 365 (2015) 57–69.
- [17] H. Dzinun, M.H.D. Othman, A.F. Ismail, M.H. Puteh, M.A. Rahman, J. Jaafar, Performance evaluation of co-extruded microporous dual-layer hollow fiber membranes using a hybrid membrane photoreactor, *Desalination*, 403 (2017) 46–52.
- [18] X. Meng, X. Gong, Y. Yin, N. Yang, X. Tan, Z.F. Ma, Effect of the co-spun anode functional layer on the performance of the direct-methane microtubular solid oxide fuel cells, *J. Power Sources*, 247 (2014) 587–593.
- [19] X.L. Zhang, C.F. Xiao, X.Y. Hu, X. Jin, Q.Q. Bai, Study on the interfacial bonding state and fouling phenomena of polyvinylidene fluoride matrix-reinforced hollow fiber membranes, *Desalination*, 330 (2013) 49–60.
- [20] X.Q. Zhang, X.Y. Fan, C. Yan, H.Z. Li, Y.D. Zhu, X.T. Li, L.P. Yu, Interfacial microstructure and properties of carbon fiber composites modified with graphene oxide, *ACS Appl. Mater. Interfaces*, 4 (2012) 1543–1552.
- [21] M.M. Haque, M.E. Ali, M. Hasen, M.N. Islam, H. Kim, Chemical treatment of coir fiber reinforced polypropylene composites, *Ind. Eng. Chem. Res.*, 51 (2012) 3958–3965.
- [22] H.L. Liu, C.F. Xiao, Q.L. Huang, X.Y. Hu, W. Shu, Preparation and interface structure study on dual-layer polyvinyl chloride matrix reinforced hollow fiber membranes, *J. Membr. Sci.*, 472 (2014) 210–221.

- [23] X.T. Zhao, Y.L. Su, W.J. Chen, J.M. Peng, Z.Y. Jiang, Grafting perfluoroalkyl groups onto polyacrylonitrile membrane surface for improved fouling release property, *J. Membr. Sci.*, 415–416 (2012) 824–834.
- [24] X.C. Fan, Y.L. Su, X.T. Zhao, Y.F. Li, R.N. Zhang, J.J. Zhao, Z.Y. Jiang, J.N. Zhu, Y.Y. Ma, Y. Liu, Fabrication of polyvinyl chloride ultrafiltration membranes with stable antifouling property by exploring the pore formation and surface modification capabilities of polyvinyl formal, *J. Membr. Sci.*, 464 (2014) 100–109.
- [25] J. Liu, P.L. Li, Y.D. Li, L.X. Xie, S.C. Wang, Z. Wang, Preparation of PET threads reinforced PVDF hollow fiber membrane, *Desalination*, 249 (2009) 453–457.
- [26] J. Brandrup, E.H. Immergut, E.A. Grulke, *Polymer Handbook*, A Wiley-Interscience Publication, United States of America, Vol. VII, 1999, pp. 671–714.
- [27] X.Y. Hu, C.F. Xiao, S.L. An, G.X. Jia, Study on the interfacial micro-voids of poly(vinylidene difluoride)/polyurethane blend membrane, *J. Mater. Sci.*, 42 (2007) 6234–6239.
- [28] X.Y. Hu, Y.B. Chen, H.X. Liang, C.F. Xiao, Preparation of pressure responsive hollow fiber membrane by melt-spinning of polyurethane-poly(vinylidene fluoride)-poly(ethylene glycol) blends, *Mater. Manuf. Process*, 25 (2010) 1018–1020.